Blocking of Steady Circulation by Coastal Geometry

ÜMIT ÜNLÜATA, TEMEL OĞUZ AND EMIN ÖZSOY

Middle East Technical University, Institute of Marine Sciences, P.K. 28, Erdemli, İçel, Turkey

(Manuscript received 23 November 1982, in final form 1 March 1983)

ABSTRACT

Along the southern Turkish continental shelf, the intensity of the observed mean flow has a considerable degree of variability. The relatively strong currents along the straight portion of the coast is reduced significantly in the nearshore region upon encountering irregularities in the form of bays and headlands. As a possible explanation of such blockage by coastal irregularities, a linear, homogeneous, wind-stress free model is presented incorporating the constraints of topographic steering and linear bottom friction. Solutions are given for an idealized case of an abrupt indentation on a straight coast adjoining a linearly deepening shelf. The directional preference of blocking and the applicability of boundary layer approximations are discussed. Numerical solutions are obtained for the realistic bathymetry and coastal configuration along the southern Turkish continental shelf. The concepts developed are applied to the observed blocking features.

1. Introduction

A cyclonic circulation in the eastern Mediterranean has been proposed as a dominant mean current system (Wüst, 1961; Lacombe and Tchernia, 1972). Accordingly, the steady surface current follows the coasts of Israel, Lebanon and Syria and turns west to flow along the southern Turkish coast. Using the observed density and wind fields, Ovchinnikov (1966), Engel (1967), Moskalenko (1974) and Gerges (1976) have confirmed computationally this picture of mean motion. Collins and Banner (1979) have utilized the computed geostrophic fields together with ERTS imagery and secchi depth measurements to provide the details of the flow in the northeastern corner of the Levantine basin. The patterns of the subsurface flow essentially follow that of the surface motion (Gerges, 1976).

Recent observations (Ünlüata *et al.*, 1978, Ünlüata *et al.*, 1980) confirm the existence of a mean westerly motion along the southern Turkish coast. These observations were made at station E2 off Erdemli (Fig. 1a). Additional long term current data obtained (unpublished) at the same station during 1980 provides further confirmation of the existence of the steady flow with velocities of the order of 10 cm s^{-1}.

While the westerly mean flow is detectable off the relatively smooth coastline extending from Mersin to Göksu river (Fig. 1a), its magnitude is found to be significantly reduced in the nearshore areas west of the Göksu river delta. In particular, during 1977–78 nearly a year-long, and in 1980 a four-month current measurement program was carried out at station A2 (Figs. 1a, b). The maximum observed mean flow was less than 4 cm s^{-1} in magnitude during all measurement periods, and there was no predominant direction. In 1980, the data collection at A2 was simultaneously carried out with that of E2. During this period the four-month average of the currents measured at E2 was near 15 cm s^{-1} while that at A2 was nearly zero.

A summary of current measurements in stations A2 and E2 with observed mean values are given in Table 1. The coordinates to which mean currents are referred are shown in Figs. 1a, b (the current components in station E2 have been aligned with the coastline). The overall mean values (statistical average weighted by data length) show that mean currents in station A2 are virtually non-existent, while in station E2 a south-westerly mean current of 7.5 cm s^{-1} is aligned with the isobaths. During the period 26 August 1978–31 January 1979, current-meters deployed continuously show reversals in the direction of mean current at E2 due to (Ünlüata, 1982) very low frequency oscillations (some periods larger than individual record lengths), but they too have a southwesterly mean of 4.3 cm s^{-1}. The better set of observations that can be used to compare station E2 with station A2 is the 1980 measurements, indicating mean southwesterly currents at 13.7 cm s^{-1} in station E2 and mean currents of less than 4 cm s^{-1} in station A2.

A distinguishing feature of the coastline between the Göksu River delta and Anamur is its ruggedness, reflecting the presence of a series of bays and headlands. The reduction in the intensity of mean motion along this segment of the coast evidently implies a significant amount of blockage of the flow by the well-

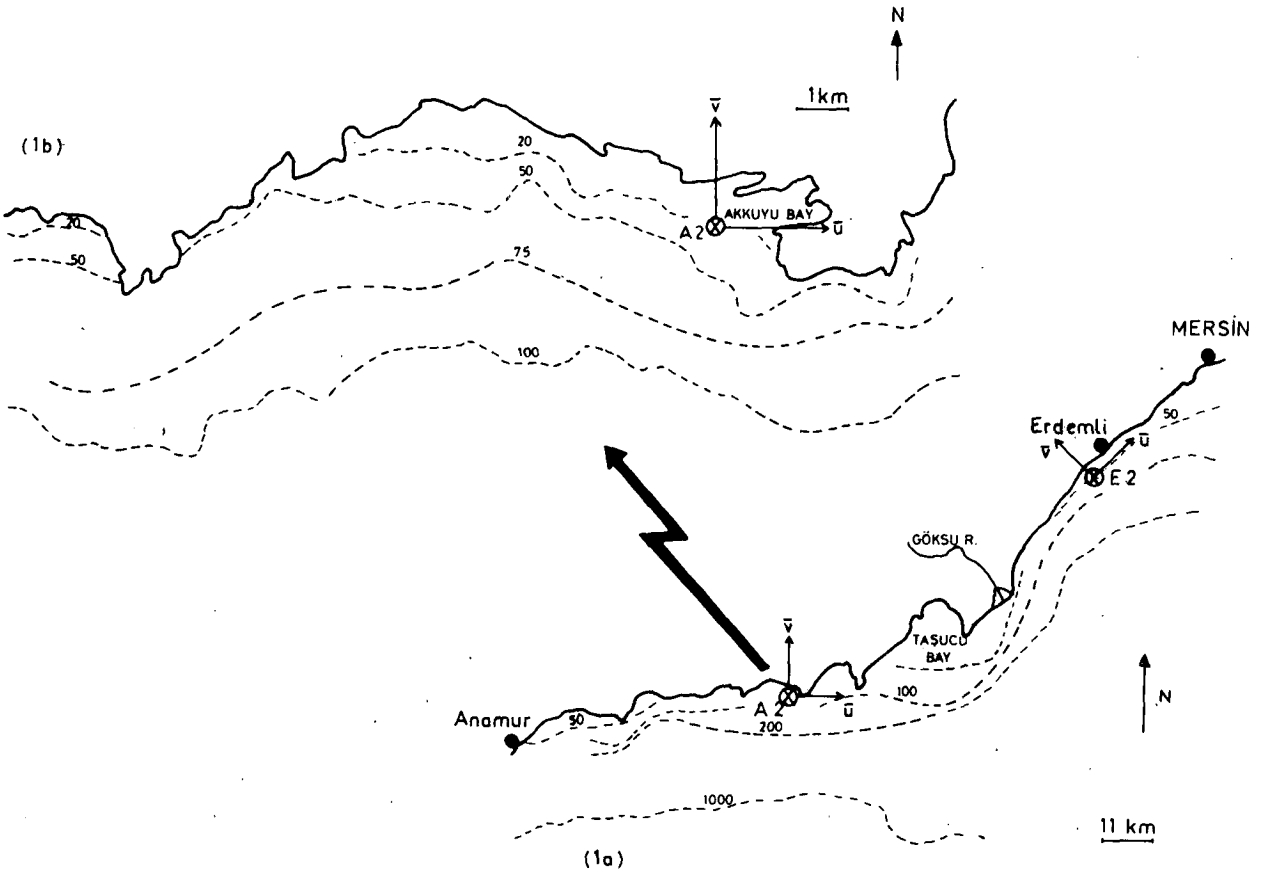

FIG. 1. Location maps.

pronounced coastal features. In particular, station A2 is located within a bay and to the west of a headland (Figs. 1a, b).

The blockage of the mean flow as far as the location of A2 is concerned may come about for various reasons. An earlier offshore deflection of the flow by the coastal perturbations on the east of A2 could lead to an effective blockage. On the other hand, the headland on the east may induce flow separation, leading to the formation of an eddy in the bay and a dead water area around A2.

Here we examine another possibility emerging from the fact that the steady flows free of wind stress tend to follow isobaths. Consider the simplest situation involving a single bay located on a coast with rapidly increasing water depth so that the coastline essentially acts as a vertical wall of height H_0 except in the bay area (Fig. 2). Within the bay, the water depth decreases from H_0. Now, in the absence of external and frictional forces, the water column moving along the coastline must preserve its height status. Consequently, upon arriving at the bay it would follow the isobath of value H_0, the flow penetrating only partially into the bay area. The vertical fluid column along the H_0 isobath thus acts as if it were a rigid barrier and the water mass in the dotted area in Fig. 2 stays stationary.

The form of blockage that is envisioned here constitutes just another result of the Taylor–Proudman theorem (Greenspan, 1968). We also note that if the other coastal perturbations are ignored, the situation depicted in Fig. 2 is sufficiently well approximated by the bay shown in Fig. 1b, where the water depth very rapidly attains a value of the order of 50 m off the headlands on the east and the west.

The lateral and the bottom frictional effects will undoubtedly influence the blockage arising as a result of the steering along isobaths. Especially, the competition between the lateral friction and the adverse pressure gradients is expected to lead to the separation of the approach flow. It is felt, however, that for sufficiently low intensity motions, the topographic effect will dominate the tendency of the flow to separate.

We study the blockage induced through topographic constraints by neglecting the horizontal diffusion of momentum but retaining the bottom friction (Section 2 and 3). An idealized case involving an abrupt semi-infinite intendation on an otherwise straight coastline (Fig. 3) is utilized to demonstrate the flow blockage in terms of analytical solutions

TABLE 1. Mean currents.

Measurement period (month/day/year)	Data length (h)	Depth (m)	Mean current (cm s^{-1}) $\bar{u}$	$\bar{v}$	
		Station A2 (Akkuyu)			
8/23/77–9/11/77	490	5	0.4	−0.1	
8/23/77–10/14/77	1231	15	−0.2	0.2	
10/2/77–10/23/77	513	5	1.1	1.0	
10/24/77–12/12/77	1153	15	−0.5	−0.2	
2/13/78–3/14/78	746	5	3.3	2.1	
2/13/78–3/14/78	746	15	0.3	1.9	
4/9/78–5/13/78	856	5	0.3	−4.1	
4/9/78–5/13/78	826	5	−0.6	−1.0	
5/18/78–6/19/78	806	5	−2.7	−0.9	
5/18/78–6/19/78	860	15	−1.3	−0.8	
6/19/80–9/4/80	1878	20	−0.7	2.2	
6/19/80–9/20/80	2269	20	−2.0	3.5	
	Overall mean:		−0.5	0.9	
		Station E2 (Erdemli)			
3/22/78–4/6/78	363	5	−8.3	0.3	
3/22/78–4/6/78	363	10	−4.6	0.2	
8/26/78–9/29/78	822	10	−9.4	−1.2	
10/4/78–10/30/78	628	15	0.9	1.2	
11/7/78–12/1/78	590	15	4.4 (−4.3)	1.7 (0.5)	
12/9/78–12/29/78	504	15	−12.7	0.6	
12/31/78–1/31/79	768	15	−4.4	0.6	
6/6/80–8/19/80	1777	20	−13.7	0.1	
	Overall mean:		−7.5	0.3	

(Section 3c). Numerical solutions relevant to the regional setting will then be provided in Section 4.

2. Formulation

We consider linear, barotropic motions taking place over variable topography on an f-plane. Forcing by wind and the effect of lateral friction will be neglected. The bottom friction is assumed to be linearly proportional to the velocity. The depth integrated equations of motion are then of the form

$$\left.\begin{aligned} f\mathbf{k}\times\mathbf{u} &= -g\nabla\eta - r\mathbf{u}/H \\ \nabla\cdot(H\mathbf{u}) &= 0 \end{aligned}\right\}, \qquad (2.1a, b)$$

where $\mathbf{u}$ is the averaged horizontal velocity, f the Coriolis parameter, $\mathbf{k}$ the unit vector along the vertical, g the gravitational constant, η the free surface displacement, r the frictional constant, H the depth and ∇ is the horizontal gradient operator.

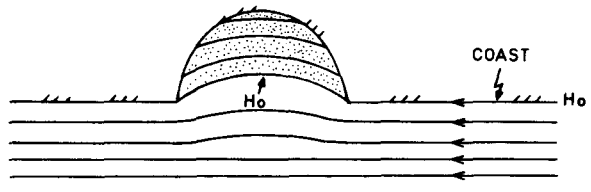

FIG. 2. Topographically induced blockage. Flow approaches from right. Solid lines imply the isobaths.

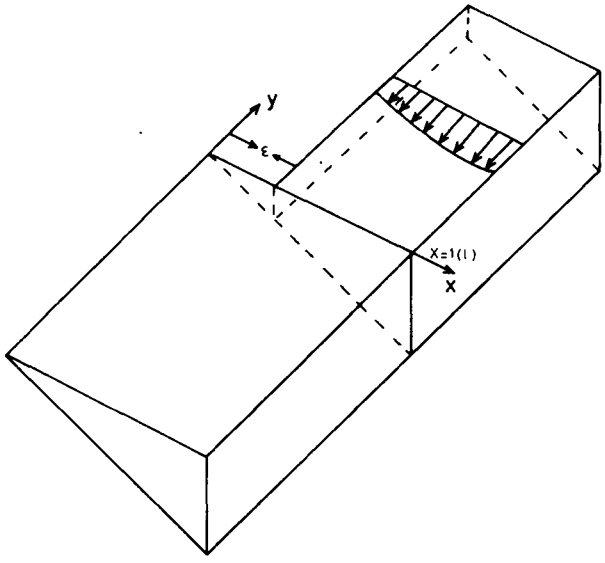

FIG. 3. A semi-infinite indentation on a coastline.

Eq. (2.1b) allows the introduction of a stream function such that

$$H\mathbf{u} = -\mathbf{k}\times\nabla\Psi \qquad (2.2)$$

and a single scalar equation for Ψ can then be obtained from (2.1a), i.e.,

$$f\nabla H\cdot\mathbf{k}\times\nabla\Psi = r(\nabla^2\Psi - 2\nabla\Psi\cdot\nabla H/H). \qquad (2.3)$$

This is the vorticity equation of motion, expressing simply the static balance between the vorticity induced because of the changes in the height of a fluid column and the frictional torques exerted by the bottom.

If the bottom friction were negligible, the right-hand side of (2.3) would vanish, implying that $\nabla H\cdot\mathbf{u} = 0$, i.e., the motion is then directed along isobaths and the height of each water column is therefore preserved. If this were the case, the water mass in the dotted area in Fig. 2 would be completely stationary. The presence of bottom friction will augment a complete blockage in accordance with (2.3).

The extent in which the bottom friction will influence a complete blockage can be demonstrated by studying the relatively simple situation depicted in Fig. 3. This will be done after some general features of the solutions of (2.3) as applied to the flows in a channel are considered.

3. Analytical solutions

a. General features

In this section we first consider some general features of wind-stress free motions occurring in a chan-

nel of width l. The water depth is assumed to vary only in the transverse direction x (Fig. 4). The steady vorticity equation (2.3) can then be cast into the following dimensionless form

$$-\alpha\Psi_y + \gamma\Psi_x = \tfrac{1}{2}\nabla^2\Psi, \tag{3.1}$$

where

$$\alpha = H_x(fH_0/2r), \quad \gamma = H_x/H. \tag{3.2a, b}$$

In obtaining (3.1) the variables $[(x, y), H, \Psi]$ have been scaled by $\{l, H_0, V_0H_0l\}$ with V_0 being the scale of the velocity field $\mathbf{u}$, and H_0 being an appropriately chosen depth.

It is an easy task to show that, the solution of (3.1) that is independent of the longshore coordinate y, is of the form

$$\Psi_\infty = C\int_0^x H^2dx.$$

The constant of proportionality C can be found in terms of the discharge Q, and in dimensionless variables Ψ_∞ reads

$$\Psi_\infty = Q\left(\int_0^x H^2dx\right)\Big/\left(\int_0^1 H^2dx\right). \tag{3.3}$$

In particular, the values of Ψ_∞ on $x = 0$ and $x = 1$ are zero and Q, respectively. The solution expressed by (3.3) is valid for arbitrary $H(x)$ and implies a basic asymptotic state in which the motion occurs only in the y-direction, the transverse component u being zero. The corresponding longitudinal component is proportional to depth, implying intensification in the deeper sections of the channel.

Consider now the general problem in which interest lies with the motions occurring in the semi-infinite region $y < 0$ when an arbitrary along-shore velocity $v_0(x)$ is prescribed on $y = 0$ and $0 < x < 1$ in terms of Ψ as

$$\Psi_0(x) \equiv \Psi(x, 0) = \int_0^x v_0(x)H(x)dx. \tag{3.4}$$

It is worth noting that $\Psi_0(0) = 0$, while $\Psi_0(1) = Q$, and these values agree with those for Ψ_∞. Clearly, the flow prescribed on $y = 0$ will be perturbed, unless $\Psi = \Psi_\infty$ on $y = 0$ in which case the only solution of (3.1) satisfying (3.4) and the boundary conditions on $x = 0, 1$ is given everywhere by Ψ_∞. In the general case when Ψ_0 differs from Ψ_∞, the asymptotic state reached by Ψ as $y \to -\infty$ is Ψ_∞. We must set

$$\Psi = \Psi_\infty + \tilde{\Psi}, \tag{3.5}$$

with the function $\tilde{\Psi}$ describing the perturbations from the basic state and satisfying

$$\begin{aligned} &-\alpha\tilde{\Psi}_y + \gamma\tilde{\Psi}_x = \tfrac{1}{2}\nabla^2\tilde{\Psi}, \\ &\tilde{\Psi} = 0 \quad \text{on} \quad x = 0, 1, \\ &\tilde{\Psi} = \Psi_0 - \Psi_\infty \equiv F(x) \quad \text{on} \quad y = 0, \\ &\tilde{\Psi} \to 0 \quad \text{as} \quad y \to -\infty. \end{aligned} \tag{3.6a–d}$$

If the problem were posed for the domain $y > 0$, then (3.5) and (3.6) still apply but now $\tilde{\Psi}$ must vanish as $y \to +\infty$.

Analytical solutions of the boundary value problem defined by Eq. (3.6) can be obtained by assuming the water depth to vary linearly with x. For such changes in depth, (3.6) is separable and the solutions can be found without invoking the boundary layer approximation that $\Psi_{xx} \gg \Psi_{yy}$. This will enable us to demonstrate explicitly a fundamental directional asymmetry, namely that unless the shallower depth is to the right of the flow, the boundary layer approximation cannot be utilized. Actually, this fact is implicitly imbedded in the character of the governing equation. When the right-hand side of (3.6a) is replaced by Ψ_{xx} the equation becomes parabolic. The problem is then ill posed in the domain $y < 0$ if $\alpha < 0$, and in the domain $y > 0$ if $\alpha > 0$. In an investigation of arrested topographic waves Csanady (1978) has encountered a similar situation, for his assumptions essentially amount to the boundary layer approximation. In a model of the flow of an estuary onto a continental shelf, Beardsley and Hart (1978) have in particular examined the motions generated by a source located on a straight coast discharging into a semi-infinite ocean. It is shown that the boundary layer approximation leads to a source solution that is (for the Northern Hemisphere) valid in the region lying to the right of the source (looking out onto the shelf) and the flow spreads by taking the shallower depth to its right. When the full equation is used, the solution valid for the entire half-space is obtained and it reveals that there exists a degree of asymmetry in the spread of the source depending on the parameter (fH_0/r). For small values of this parameter the source spreads symmetrically into the two quadrants of the half-space. Typically, however, $fH_0r^{-1} \gg 1$ and the flow favors spreading towards right. It is worth pointing out that we can infer this type of source behaviour directly from the governing Eq. (3.1). The equation is similar to the convective–diffusion equation with $-\alpha$ and γ standing for the "velocities" in the y and x directions, respectively. In this analogy then boundary layers will develop only

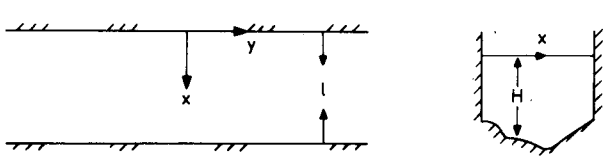

FIG. 4. Definition sketch for channel flows.

for sufficiently large values of $-\alpha$ viz., proportional to fH_0/r.

We now proceed to discuss the aforementioned type of asymmetry as it is related to the present problem. The salient aspects of this asymmetry will then be utilized in studying the blockage problem in an idealized situation.

b. The channel flow

Consider the boundary value problem (3.6) when the dimensionless water depth varies as $H = x$. Then $\alpha = fH_0/2r$ and $\gamma = x^{-1}$, with H_0 standing for the water depth along the coast on $x = 1$. The water depth on $x = 0$ could be taken non-zero but this does not influence the features to be demonstrated.

The solution to equation (3.6) is easily found to be of the form

$$\tilde{\Psi} = \sum_{n=1}^{\infty} A_n \psi_n(x) \phi_n^{<}(y), \tag{3.7a}$$

where the functions

$$\psi_n = \sin \lambda_n x - \lambda_n x \cos \lambda_n x \tag{3.7b}$$

form an orthogonal set in the sense that

$$\int_0^1 x^{-2} \psi_n \psi_m dx = \begin{cases} 0, & n \neq m \\ \tfrac{1}{2}\lambda_n^2 \sin^2 \lambda_n, & n = m \end{cases} \tag{3.7c}$$

with the eigenvalues λ_n being determined by the roots of

$$\tan \lambda = \lambda. \tag{3.7d}$$

In (3.7a) the functions ϕ_n are evanescent in y and are given by

$$\phi_n^{<} = \exp\{y[-\alpha + (\alpha^2 + \lambda_n^2)^{1/2}]\}, \quad y < 0, \tag{3.7e}$$

while the coefficients A_n are found by utilizing (3.7c).

$$A_n = \frac{2 \int_0^1 x^{-2} \psi_n(x) F(x) dx}{\lambda_n^2 \sin^2 \lambda_n}. \tag{3.7f}$$

If the problem is posed for the domain $y > 0$, then the solution is still given by (3.5) but the function $\phi^{<}$ appearing in (3.7a) must be replaced by

$$\phi_n^{>} = \exp\{-y[\alpha + (\alpha^2 + \lambda_n^2)^{1/2}]\}, \quad y > 0. \tag{3.8}$$

Consider first now the solution that is valid in $y < 0$. It is seen that the decay of the nth mode of the perturbation stream function $\tilde{\Psi}$ is measured by the normalized distance

$$y^{(n)} = [(\alpha^2 + \lambda_n^2)^{1/2} - \alpha]^{-1}. \tag{3.9a}$$

The parameter $\alpha = fH_0/2r$ is typically much greater than unity. Assuming the predominance of the first few modes of $\tilde{\Psi}$, $\lambda_n = O(1)$ and it therefore follows from (3.9a) that

$$y^{(n)} \approx 2\alpha/\lambda_n. \tag{3.9b}$$

Consequently, the development of the flow to Ψ_∞ occurs within distances much greater than the channel width. Moreover, it is a simple task to show that $v = -H^{-1}\tilde{\Psi}_x = O(1)$ while $u = H^{-1}\tilde{\Psi}_y = O(1/\alpha) \ll v$. Therefore, the boundary layer approximation for the problem in $y < 0$ would have been appropriate.

Considering next the problem posed for $y > 0$, we infer from (3.8) that the decay of $\tilde{\Psi}$ would occur, for $\alpha \gg 1$ and $\lambda_n = O(1)$, within a distance

$$y^{(n)} \approx \tfrac{1}{2}\alpha. \tag{3.10}$$

This implies a decay distance of the order of one percent of the channel width, i.e., the rapid variations occur in the direction of the flow. When the problem is posed for $y > 0$ the boundary layer approximation hence fails. Moreover, consistent with this failure we can show that $u = O(\alpha)$ and $v = O(1)$.

The fact that the motion very rapidly decays to the basic state for the region $y > 0$ has important ramifications with regard to the blockage problem to be studied next.

c. Blockage problem

Consider the following idealized problem involving the interaction of a wind-stress free flow with an abrupt semi-infinite indentation on an otherwise straight coast bounding the offshore extent of the water mass at a distance l ($x = 1$ in dimensionless units) which is qualitatively identified as a shelf width. The flow approaches the coastal transition from the $+y$ direction. In the region of $y > 0$ the shelf terminates at a coastal wall, while in the region $y < 0$ the depth vanishes at the coast. We assume that the approach flow is in the basic state, i.e., it is given, as $y \to +\infty$, by

$$\Psi_\infty^{>} = \frac{Q \int_\epsilon^x H^2(x) dx}{\int_\epsilon^1 H^2 dx}, \tag{3.11}$$

Q being the discharge.

The exact solution of the problem just posed is obtainable by first considering the regions $y > 0$ and $y < 0$ separately and matching the solutions later on the common boundary $y = 0$ (by requiring the continuity of pressure and the velocity components v). This procedure leads to an integral equation which is solvable by variational or numerical techniques. Instead of doing this we utilize the results of the earlier problem as follows.

In $y < 0$ the solution is given by (3.5) and (3.7) with $F(x)$ left yet unspecified and Ψ_∞ being determined through (3.3).

In the region $y > 0$, the solution is given by the superposition of (3.11) and (3.7a) with the understanding that $\phi_n^<$ are to be replaced by $\phi_n^>$. However, the functions of $\phi_n^>$ rapidly decay so that in effect the value of the stream function Ψ on $y = 0$, i.e., Ψ_0 is given by (3.11) in $\epsilon < x < 1$ while $\Psi_0 = 0$ in $0 < x < \epsilon$.

Consequently, from Eq. (3.6c),

$$F(x) = \begin{cases} -\Psi_\infty(x) & , \quad 0 < x < \epsilon \\ \Psi_\infty^>(x) - \Psi_\infty(x) , & \epsilon < x < 1 \end{cases} \tag{3.12}$$

with Ψ_∞ and $\Psi_\infty^>$ being given by (3.3) and (3.11), respectively. Eq. (3.12) specifies $F(x)$ and therefore the streamfunction $\tilde{\Psi}$ through (3.7a–f). For $H = x$, the complete solution (3.5) is found to be

$$\Psi = x^3 - \frac{6}{(1-\epsilon^3)} \sum_n \frac{\psi_n(x)\psi_n(\epsilon)\phi_n^<(y)}{\lambda_n^4 \sin^2\lambda_n}, \tag{3.13}$$

wherein we have set $Q = 1$.

It is important to note that (3.13) implies vanishing longshore velocity $v = -\Psi_x/H$ on $x = 0$. Consequently, it is expected that the horizontal diffusion of vorticity plays a minor role. We further note from (3.13) that in the absence of bottom friction complete blockage would occur in the region $x < \epsilon$. The role of bottom friction on the amount of blockage of the mean flow is deduced from (3.13) by varying the value of nondimensional parameter α. The results for different α values and for the case of $\epsilon = 0.25$ are depicted in Fig. 5. The streamline pattern corresponding to $\alpha = 100$ shows a significant amount of blockage along the coastline at $x = 0$ for the region $y < 0$. The increase in the bottom friction of almost one order of magnitude (i.e., $\alpha = 10$) still shows a considerable amount of blockage along the coastline without affecting the interior geostrophic flow pattern. Finally, the parameter ϵ reflects the amount of blockage in the sense that larger ϵ characterizes the region where more blockage might occur for the flow

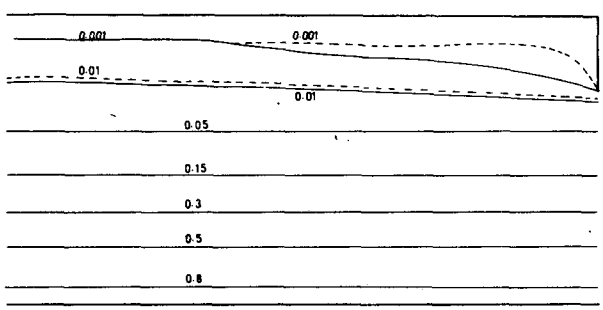

FIG. 5. The streamline pattern for a semi-infinite indentation on a coastline with $\epsilon = 0.25$. Continuous line corresponds to $\alpha = 100$, broken line to $\alpha = 10$.

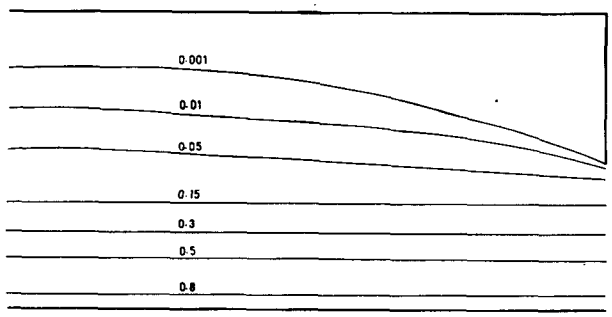

FIG. 6. As in Fig. 5, but for $\epsilon = 0.5$ and $\alpha = 100$.

approaching to the region. This is evident by comparing Figs. 5 and 6, the latter corresponding to the case of $\epsilon = 0.5$.

4. Numerical solutions

This section deals with the topographically controlled blockage of the mean flow along the southern Turkish coastal waters between the Göksu River delta and Anamur. The region has a complex coastal geometry associated with a series of bays and headlands and is further characterized by the presence of a steep and narrow shelf with rapid deepening to 1000 m in ~10–15 km offshore (Fig. 1a).

Considering that the cross-shelf depth variations are sufficiently rapid along the coast under study, topographic effects on the flow dominate and lateral diffusion effects become relatively unimportant. The wind-stress free mean circulation driven by the large-scale steady currents of the northeastern Levantine Sea is then described by numerical solution of Eq. (2.3).

The model incorporates realistic bathymetry of the shelf region. A false constant bottom is however, assumed for places deeper than 300 m, in a region 36 km wide in the offshore direction. The offshore extent of the region being modelled is terminated by a vertical wall across which the normal flow is set to zero as being consistent with the assumption of geostrophic balance.

Eq. (2.3) is discretized in a rectangular mesh of grid spacing $\Delta y = \Delta x = 3.0$ km in the longshore and transverse directions, respectively. The value $r = 0.003$ m s^{-1} is assumed for the linear bottom friction coefficient. Coriolis parameter takes the value $f = 1.0 \times 10^{-4}$ s^{-1} and gravitational acceleration $g = 9.81$ m s^{-2}. The vorticity equation (2.3) is solved for the boundary condition prescribed at the eastern open-boundary according to Eq. (3.4). The solution procedure is the Gauss–Seidel iterative method described by Ramming and Kowalik (1980).

The mean circulation in the shelf region driven by

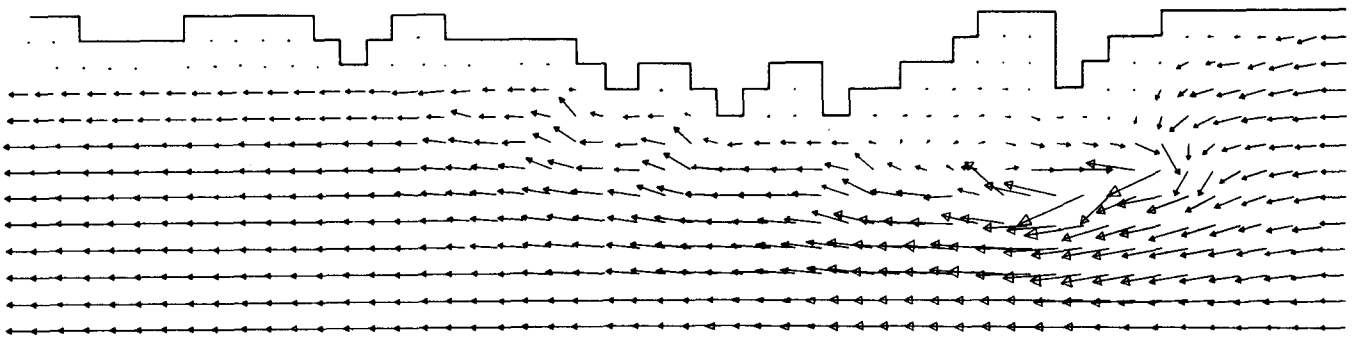

FIG. 7. The depth-averaged steady circulation in the southern Turkish continental shelf.

the large scale current system of Levantine Sea is shown on Fig. 7. The flow, which is almost in a geostrophic balance and tends to follow isobaths along the continental shelf, penetrates only partially into the bay areas due to topographic steering and leads to the aforementioned blockage. The situation is clearly shown within Taşucu Bay where the flow following the 100 m isobath is deflected partially into the bay to set up a weak clockwise circulation. Further experiments have confirmed that the bottom friction as well as rotation and lateral friction have a minimal influence on the circulation developed.

5. Summary and conclusions

A linear, barotropic model of wind-stress free steady motions on a shelf has been used in an attempt to explain the observed blocking of mean flow near coastal irregularities on the southern Turkish continental shelf. In geostrophic flow, regions with closed depth contours near the coast (such as bays of Fig. 2) should be completely blocked off from the mainstream flow on the shelf, but such solutions are indeterminate. To remove geostrophic indeterminacy, linear bottom friction has been introduced in the present linear model, although it may be noted that nonlinear advection terms have been kept in other applications (for example: Charney and De Vore, 1979). Nonlinear processes such as advection, flow separation at coastal boundaries and nonlinear bottom friction have not been taken into account on the basis of sufficiently weak mean currents.

In this model, vorticity changes induced by motions across depth contours are exactly balanced by torques applied by the bottom shear stress. Analytical solutions require that the currents on the shelf evolve into asymptotic states [Eq. (3.3)] and that this evolution has fundamental asymmetry. Consequently, boundary layer approximation may only be invoked if the shallower depth is to the right of the approaching flow.

The behavior of the flow can be directly explained utilizing Eq. (3.1) which is analogous to the convective diffusion equation with $-\alpha$ and γ standing for the convective velocities in the y and x directions, respectively. In this analogy, for $H_x < 0$, there exists the competitive effects of diffusion (which will tend to smear an initial profile in x, y) and convection in $-y$ and x directions. For sufficiently large values of α, boundary layers will develop in the region $y < 0$. Consider, for example, an approaching channel flow with zero initial vorticity specified at $y = 0$. Since the bottom stress (last term in 2.1a) is larger for shallower depths a negative bottom torque will be applied on the fluid, which will therefore deflect towards deeper water to balance this effect. Two boundary layers will develop along $x = 0$ and $x = 1$ in $y < 0$, and the flow will be pumped from one to the other boundary layer until the basic state (3.3) is reached within distances much greater than the channel width. In $y > 0$, the boundary layer approximation cannot be used due to directional asymmetry, and the flow reaches its eventual basic state only within a few percent of the width scale of the channel. Advantage is taken of this fact in Section 3 so that the basic state has been specified for $y > 0$ in solving the coastal indentation problem.

The solutions show how bottom friction augments the geostrophic blockage near coastal and topographic irregularities, though the effects of friction do not avoid blockage in a complete sense. While these conclusions are only valid in the absence of lateral diffusion of momentum and nonlinear effects, numerical experiments performed in investigating the flow structure of the southern Turkish continental shelf have verified that these effects are indeed negligible so far as blocking is influenced to any extent.

REFERENCES

Beardsley, R. C., and J. Hart, 1978: A simple theoretical model for the flow of an estuary onto a continental shelf. *J. Geophys. Res.*, **83**, 873–883.

Charney, J. G., and J. G. DeVore, 1979: Multiple flow equilibria in the atmosphere and blocking. *J. Atmos. Sci.*, **36,** 1205–1216.

Collins, M. B., and F. T. Banner, 1979: Secchi disc depths, suspensions and circulation, northeastern Mediterranean Sea. *Mar. Geol.*, **31,** M39–M46.

Csanady, G. T., 1978: The arrested topographic wave. *J. Phys. Oceanogr.*, **8,** 47–62.

Engel, I., 1967: Currents in the eastern Mediterranean. *Int. Hydrogr. Rev.*, **44,** 23–40.

Gerges, M. A., 1976: Preliminary results of a numerical model of circulation using the density field in the eastern Mediterranean. *Acta Adriat.* **18,** 165–176.

Greenspan, H. P., 1968: *The Theory of Rotating Fluids*, H. P. Greenspan, Ed. Cambridge University Press, 329 pages.

Lacombe, H., and R. Tchernia, 1972: Characterés hydrologiques et circulation des eaux on Méditerranée. *The Mediterranean Sea,* Dowden, Hutchison and Ross, 25–36.

Moskalenko, L. V., 1974: Steady-state wind-driven currents in the eastern half of the Mediterranean Sea. *Oceanology,* **14,** 491–494.

Ovchinnikov, I. M., 1966: Circulation in the surface and intermediate layers of the Mediterranean. *Oceanology,* **5,** 48–58.

Ramming, H. G., and Z. Kowalik, Ed., 1980, *Numerical Modelling of Marine Hydrodynamics.* Elsevier, 368 pp.

Ünlüata, Ü., 1982: On the low-frequency motions in the Cilician Basin. *J. Phys. Oceanogr.*, **12,** 134–143.

——, M. A. Latif, F. Bengü and H. Akay, 1978: Towards an understanding of shelf dynamics along the southern coast of Turkey, IV^{es}. *J. Etud. Pollut.*, Antalya, Comm. Inter pour L'Exploration Scientifique de la Mer Méditerraneé, 535–542.

——, E. Özsoy and M. A. Latif, 1980: On the variability currents in the northeastern Levantine Sea, V^{es}. *J. Etud. Pollut.*, Cagliari, Comm. Inter pour L'Exploration Scientifique de la Mer Méditerraneé, 929–936.

Wüst, G., 1961: On the vertical circulation of the Mediterranean Sea. *J. Geophys. Res.*, **66,** 3261–3271.